Original Article

Mol Imaging Radionucl Ther *DOI:10.4274/mirt.galenos.2025.77200 [Epub Ahead of Print]*

Investigation of the Partial Volume Effect in Pre-Dosimetry of Liver Tumors for ^{90}Y Radioembolization: A Phantom Study

^{90}Y Radyoembolizasyon Tedavisinde Karaciğer Tümörleri Pre-Dozimetri'de Kısmi Hacim Etkisinin İncelenmesi: Bir Fantom Çalışması

Ayşe Dilaver Akar[1], Nami Yeyin[2], Sinem Akyol[2], Özge Demir[3], Eylem Gülce Çoker[1], Mustafa Demir[2]

[1]*İstanbul Aydın University, Graduate Education Institute, Health Physics Program, İstanbul, Türkiye*
[2]*İstanbul University-Cerrahpaşa, Cerrahpaşa Faculty of Medicine, Department of Nuclear Medicine, İstanbul, Türkiye*
[3]*İstanbul University-Cerrahpaşa, Cerrahpaşa Faculty of Medicine, Department of Chemical Engineering, İstanbul, Türkiye*

Abstract

Objectives: Yttrium-90 (^{90}Y) radioembolization has become increasingly important in the treatment of liver tumors. This study aims to experimentally determine the extent to which small liver tumors are affected by the partial volume effect (PVE) in single photon emission computed tomography/computed tomography (SPECT/CT) scintigraphy using technetium-99m-macroaggregated albumin (Tc-99m-MAA), and to investigate the impact of PVE on tumor dosimetry and image quality.

Methods: In this experimental study, a custom-designed liver phantom containing four tumor mimics with diameters of 1 cm, 2 cm, 3 cm, and 5 cm was used. The tumor and liver parenchyma volumes were filled with Tc-99m at a ratio of 4.86: 1. The phantom was imaged in a water tank using SPECT/CT according to standard clinical protocols. Volumetric regions of interest were drawn for each lesion and tumor volumes, contrast values (C), contrast to noise ratios (CNR), and absorbed tumor doses were calculated from the counts obtained. Since this study does not involve live subjects and was conducted solely on a phantom model, ethical approval, informed consent, and consent forms are not required for this study.

Results: Tumor diameters measured on SPECT/CT images matched those obtained from both CT images and the actual dimensions. The contrast values calculated from the SPECT/CT images for lesions with diameters of 2 cm and 5 cm were 2.03 and 3.89, respectively. Similarly, the corresponding CNR values were 8.64 and 21.07. Tumor-to-normal tissue ratios were 2.03 and 3.89 for the 2 cm and 5 cm lesions, respectively.

For the 2 cm lesion, the actual and SPECT/CT-derived absorbed doses were 15.3 Gy and 7.87 Gy, respectively. For the 5 cm lesion, these values were 15.4 Gy and 13.38 Gy, respectively. the absorbed tumor doses significantly decreased as tumor diameter decreased due to the influence of PVE.

Conclusion: Tumors smaller than 2 cm in diameter were markedly affected by the PVE. Considering the influence of PVE, or applying appropriate corrections in dosimetric calculations, is of critical importance for improving the accuracy of dosimetry results.

Keywords: ^{90}Y radioembolization therapy, Tc-99m-MAA dosimetry, partial volume effect, tumor imaging, image quality

Address for Correspondence: Eylem Gülce Çoker, İstanbul Aydın University, Graduate Education Institute, Health Physics Program, İstanbul, Türkiye
E-mail: demirm@iuc.edu.tr **ORCID ID:** orcid.org/0000-0001-6361-9458
Received: 14.02.2025 **Accepted:** 18.06.2025 **Epub:** 13.08.2025

Cite this article as: Dilaver Akar A, Yeyin N, Akyol S, Demir Ö, Çoker EG, Demir M. Investigation of the partial volume effect in pre-dosimetry of liver tumors for ^{90}Y radioembolization: a phantom study. [Epub Ahead of Print]

Öz

Amaç: Karaciğer tümörlerine yönelik ittriyum-90 (^{90}Y) radyoembolizasyon tedavisinin önemi giderek artmaktadır. Bu çalışmanın amacı, teknesyum-99m-makroagregat albümin (Tc-99m-MAA) kullanılarak yapılan tek foton emisyonlu tomografi/bilgisayarlı tomografi (SPECT/BT) sintigrafisinde küçük karaciğer tümörlerinin kısmi hacim etkisinden (PVE) etkilenme düzeylerinin deneysel olarak belirlenmesi ve PVE'nin tümör dozları ile görüntü kalitesi üzerindeki etkisinin araştırılmasıdır.

Yöntem: Bu deneysel çalışmada, çapları 1 cm, 2 cm, 3 cm ve 5 cm olan dört taklit tümör içeren özel tasarlanmış bir karaciğer fantomu kullanıldı. Tümör/karaciğer parankim dokusunu temsil eden hacimler Tc-99m ile 4,86/1 oranında dolduruldu. Fantom, rutin klinik protokollere uygun olarak bir su tankı içinde SPECT/BT ile görüntülendi. Lezyonlardan hacimsel ilgi alanları çizilerek elde edilen sayımlardan lezyon hacimleri, kontrastlar (C), kontrast/gürültü oranları (CNR) ve tümör dozları hesaplandı.

Bulgular: SPECT/BT görüntülerinde tümör çapları, BT görüntülerinden ölçüldü ve gerçek değerlerle aynı ölçülerde bulundu. 2 cm ve 5 cm çaplı lezyonlar için SPECT/BT görüntülerinden hesaplanan kontrast değerleri sırasıyla 2,03 ve 3,89 bulundu. Benzer şekilde CNR değerleri sırasıyla 8,64 ve 21,07 bulundu. Tümör/normal doku (oranları 2 cm ve 5 cm çaplı lezyonlar için sırasıyla 2,03 ve 3,89 bulundu.

2 cm çaplı lezyon için reel ve SPECT/BT'den hesaplanan absorbe dozlar sırasıyla 15,3 Gy ve 7,87 Gy bulundu. 5 cm çaplı lezyon için reel ve SPECT/BT'den hesaplanan absorbe dozlar sırasıyla 15,4 Gy ve 13,38 Gy bulundu. PVE'ye bağlı olarak tümör çapı azaldıkça tümör dozlarının da önemli oranda azaldığı belirlendi.

Sonuç: Çapı 3 cm'den küçük olan tümörler PVE' den belirgin şekilde etkilenmiştir. Dozimetri hesaplamalarında PVE etkisinin göz önünde bulundurulması veya gerekli düzeltmelerin uygulanması, dozimetri sonuçlarının doğruluğunu artırmak açısından büyük önem taşımaktadır.

Anahtar Kelimeler: ^{90}Y mikroembolizasyon tedavisi, Tc-99m-MAA dozimetrisi, kısmi hacim etkisi, tümör görüntüleme, görüntü kalitesi

Introduction

Yttrium-90 (^{99}Y) transarterial radioembolization is an important treatment option for liver malignancies, including hepatocellular carcinoma and liver metastases originating from colorectal cancer (1,2,3). Primary and secondary liver tumors (Tm) that are not amenable to surgery can be treated through the transarterial administration of ^{99}Y-labeled microspheres. While 80-100% of liver Tm are supplied arterially via the hepatic artery, 60-70% of the normal liver parenchyma receives blood from the portal vein. When microspheres are administered via catheter into the hepatic artery, they predominantly accumulate in the peripheral areas of the tumor regions with higher perfusion thus theoretically enabling the delivery of high radiation doses to the tumor while sparing the normal parenchymal tissue.

Prior to treatment, technetium-99m-macroaggregated albumin (Tc-99m-MAA), is administered by the interventional radiology department to predict the biodistribution of ^{99}Y microspheres. Following angiography, hepatic artery perfusion scintigraphy is performed to assess any extrahepatic leakage of the radiotracer and to evaluate the distribution of radioactivity within the tumor (4,5). The Tc-99m-MAA photon emission computed tomography/computed tomography (SPECT/CT) scan, performed intra-arterially prior to ^{99}Y microsphere therapy, is used to determine the hepatopulmonary shunt fraction and to exclude potential reflux of radioactive material into the bowel, stomach, or pancreas (6). The distribution of microspheres in the capillary bed as seen on Tc-99m SPECT/CT imaging closely resembles the distribution of ^{99}Y microspheres during actual treatment; therefore, this imaging method is used in dosimetric studies (7).

Partial volume effect (PVE) is a phenomenon that arises when small lesions appear larger and with lower activity on scintigraphy due to the limited spatial resolution of the imaging system. If the imaged object or region is smaller than twice the full width at half maximum (FWHM) in the x, y, and z axes of the system, the activity within the lesion will be underestimated and its visual clarity diminished (8). PVE is a complex process influenced by several factors, including tumor size and shape, background activity in surrounding tissues, the spatial resolution of the imaging system, voxel size, and imaging modality. One of the primary causes of blurring in three-dimensional imaging is limited spatial resolution. Signal intensity within voxels represents tissue properties. Even when the spatial resolution of the imaging system is optimal, PVE may occur if lesion size is small. Additionally, smaller voxel sizes contribute to an increase in PVE (9).

The aim of this study is to: identify the perfused regions and their activity distribution in SPECT/CT scintigraphy using Tc-99m-MAA; experimentally determine the degree to which small liver Tm are affected by PVE; and investigate the impact of PVE on tumor dosimetry and image quality (IQ).

Materials and Methods

This study was conducted at the Department of Nuclear Medicine, İstanbul University-Cerrahpaşa Faculty of Medicine. The liver phantom used in the study was

designed based on the model described by Yeyin et al. (10). Additionally, lesions specific to this study were added to the phantom (Figure 1).

Liver Phantom and Water Tank

The model designed for this study consists of two main components: the liver and the water tank. The materials used in the phantom were selected in collaboration with the Department of Chemical Engineering. The liver was produced using a 3D printer and additive manufacturing technique (Fused Deposition Modeling), with a filament material called polylactic acid (PLA), which has a density of 1.24 g/cm³. Both the outer wall of the liver parenchyma and the outer shells of the simulated Tm were made of PLA, each with a thickness of 1.5 mm. The dimensions of the liver phantom are 112 mm × 191 mm, and its empty weight is 350 grams. The diameters of the four simulated lesions in the phantom are 1 cm, 2 cm, 3 cm, and 5 cm, with internal volumes that need checking against spherical volume calculations for consistency. The volume representing the liver parenchyma is 615 cm³. The second component of the phantom set, the water tank, has a depth of 20 cm and dimensions of 25 × 30 cm. The water tank and its mounting apparatus are made of Plexiglas, with no metal components used. The water filled in the tank simulates the photon scattering environment that may arise from organs and tissues other than the liver.

Phantom Operating Principle and Functionality

Our model includes four separate cylindrical tumor cavities within the liver phantom. These Tm can be filled with Tc-99m at either the same or different concentrations. Additionally, the cavity representing the liver parenchyma can be filled with a radioactive substance through a separate cap. After the phantoms are placed in the tank, they are fixed with plastic screws. Once the tank is filled with water, it can be positioned for imaging.

Imaging Protocol

SPECT/CT imaging was performed using a Siemens Symbia T16 SPECT/CT device equipped with a low-energy high-resolution collimator and dual detectors (Figure 2). After the Tm and all the compartments representing liver parenchymal tissue were filled with Tc-99m at a concentration of 2.13 µCi/mL, SPECT/CT imaging was performed. The routine clinical protocol was used for imaging. Low-dose CT scanning was performed with 120 kV and 100 mAs. The parameters used for SPECT/CT imaging were 140 keV, 15% dual-energy window, 128 × 128 matrix, 40 projections per scan, non-circular continuous orbit, and 20 seconds exposure time per SPECT projection. SPECT/CT data were reconstructed using the ordered subsets expectation maximization (3D) method with eight iterations and eight subsets. A 6 mm Gaussian filter was used for scatter correction based on the dual-energy window and attenuation correction based on CT data.

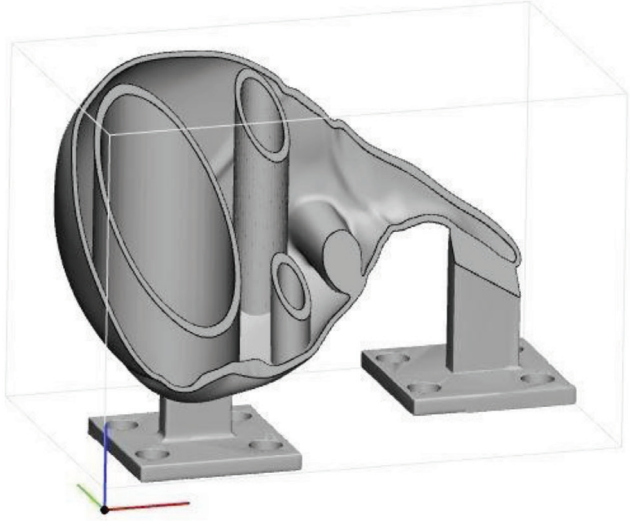

Figure 1. 3D image of the liver phantom and the fixation feet inside the water tank

Figure 2. Position of the liver phantom in the SPECT/CT device within the water tank

SPECT/CT Image Quality Quantification

To assess SPECT/CT IQ volumetric regions of interest (VOIs) were drawn on the SPECT/CT images. Based on the counts within the VOIs, tumor-to-normal tissue ratio (T/N), contrast (C), and contrast-to-noise ratio (CNR) were calculated (11).

$$C = \frac{Nl - Nbg}{Nbg} \quad (1)$$

Nl = Counts within the lesion VOI, Nbg = Counts within the background

$$CNR = \frac{C}{COV} \quad (2)$$

C: Contrast, COV: The coefficient of variation is given by

$$COV = \frac{\sigma bg}{Nbg}$$

σbg is the standard deviation of the background VOI.

Organ and Tumor Doses

Based on the activity amounts of the Tc-99m radioisotope filled into the phantom, the actual doses for both the tumor and the liver were calculated and considered as reference doses. The internal volumes of the phantom were assumed to correspond to the volume of the Tc-99m solution within the phantom. In the dosimetric calculations based on SPECT/CT images, the masses of organs and Tm were determined from CT-derived volume measurements.

The administered activity (A) was calculated using Equation 3, and the absorbed dose (D) was calculated using Equation 4 (12).

$$A\ (GBq)_{Total} = A\ (GBq)_{Normal\ liver\ tissue} + A\ (GBq)_{Tumor} \quad (3)$$

A $(GBq)_{Total}$: The amount of activity filled into the phantom's simulated lesions and the compartments representing the liver parenchymal tissue.

$$D\ (Gy)_{Tumor} = \frac{49.38\ A_{total}\ (1-LSF)}{\frac{1}{\frac{T}{N}}\left(m_{Normal\ liver\ tissue} + \frac{T}{N} m_{Tumor}\right)} \quad (4)$$

D $(Gy)_{Tumor}$: Tumor dose

LSF: Lung shunt fraction (assumed to be zero), T/N: Tumor-to-normal tissue activity ratio, m: Mass (kg)

Results

Following the filling of all compartments representing Tm and normal liver parenchyma with Tc-99m at a concentration of 2.13 μCi/mL, SPECT/CT imaging was performed. In the scintigraphic cross-sectional images obtained after scanning, the outer boundaries of the lesions were clearly visible (Figure 3). The actual tm of 1 cm, 2 cm, 3 cm, and 5 cm were found to match with the tms measured on SPECT/CT images. For CNR calculation, 12 equally sized VOIs were drawn from the SPECT/CT and Planar images shown in Figure 3. The significance between VOI counts was compared using the Mann-Whitney U test. A significant difference was found between the two VOI groups at p=0.015.

The contrast and CNR values calculated from the SPECT/CT images are presented in Table 1. The T/N activity ratios and tumor doses are shown in Table 2. Based on the actual Tc-99m activity values administered to the phantom, the

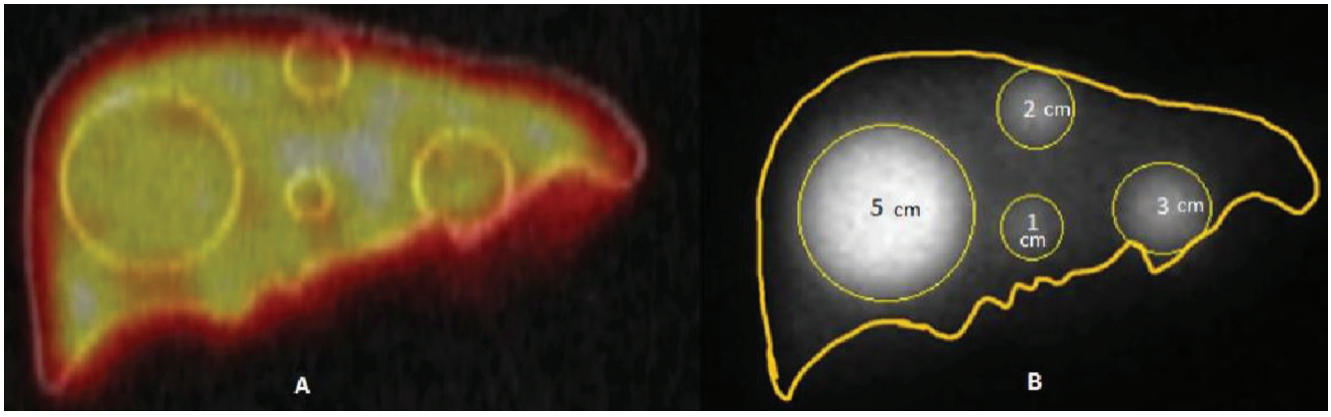

Figure 3. SPECT/CT fusion VOI images showing the CT image of the lesions (A). In the planar image, the numbers inside the ROIs represent the lesion diameters (B)

T/N ratio was kept constant at 4.86:1. However, it was observed that the T/N ratios increased with increasing tumor diameter (tm) in the SPECT/CT images. The tumor volumes calculated from the SPECT/CT images were found to be 16 cm^3, 20 cm^3, 30 cm^3, and 205 cm^3. The correlation between tumor volumes and tumor doses is presented in Figure 4.

The correlation between the tumor doses calculated from SPECT/CT images and the CNR values is shown in Figure 5. It was observed that CNR values increased with increasing tumor dose. However, for the tumor with a volume of 30 cm^3, the increase in CNR value appeared to be disproportionate compared to the others. The correlation between the tumor doses and contrast values calculated from the SPECT/CT images is presented in Figure 6. It was determined that contrast values also increased with tumor dose, and that there was a strong correlation between them.

Discussion

In this study, PVE investigation was conducted using a specially designed liver phantom that included four simulated Tm with diameters of 1 cm, 2 cm, 3 cm, and 5 cm, as well as a separate compartment representing normal liver parenchyma. In scintigraphic imaging, PVE is a well-known phenomenon that particularly affects the visibility of small-volume lesions and leads to significant errors in dosimetric calculations based on scintigraphic

Table 1. Contrast, CNR, and noise values calculated from SPECT/CT

Tumor diameter (cm)	Contrast (SPECT/CT)	CNR (SPECT/CT)
1	1.64	5.5
2	2.03	8.64
3	2.24	9
5	3.89	21.07

CNR: Contrast to noise ratio, SPECT/CT: Single photon emission computed tomography/computed tomograpy

Table 2. Lesion diameter, scintigraphic T/N ratios, and calculated tumor doses in the actual T/N (4.86/1)

Tumor diameter (cm)	T/N (SPECT/CT)	Actual doses calculated from phantom activites (Gy)	Tumor dose calculated from SPECT/CT (Gy)	Tumor dose decreas rates (%)
1	1.65	14.9	6.04	59.3
2	2.03	15.3	7.87	48.6
3	2.24	16.3	9.66	40.8
5	3.89	15.4	13.38	7.97

SPECT/CT: Single photon emission computed tomography/computed tomograp, T/N: Tumor-to-normal tissue ratio,

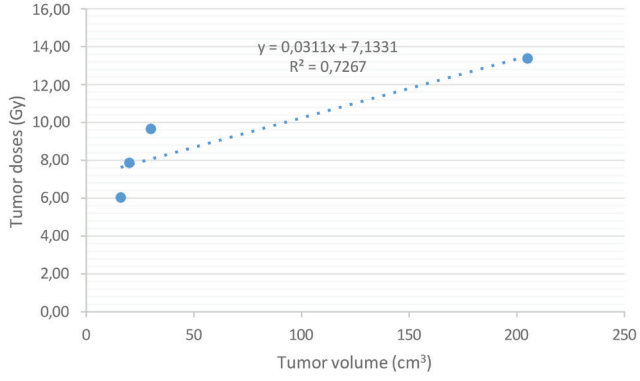

Figure 4. Tumor volume-tumor dose correlation obtained from SPECT/CT images

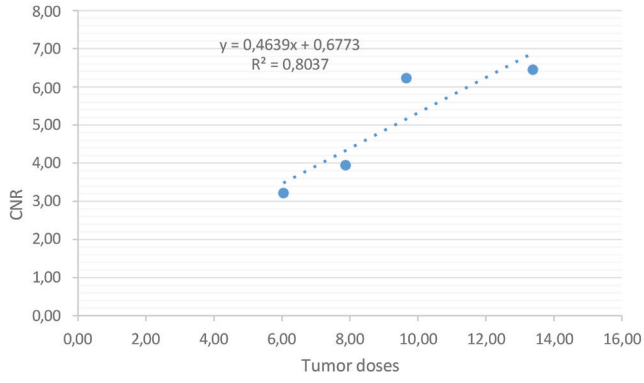

Figure 5. Tumor dose/CNR correlation calculated from SPECT/CT

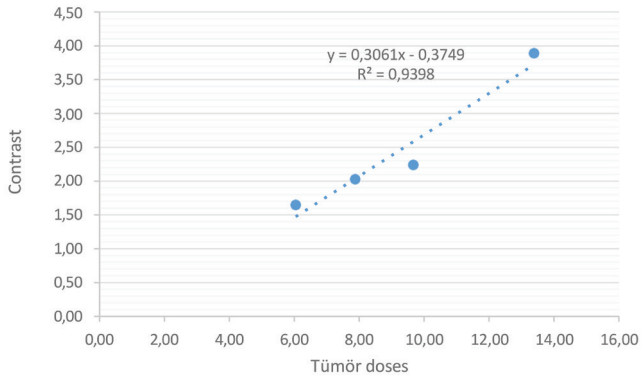

Figure 6. Tumor dose-contrast correlation in SPECT/CT

images (13,14,15). This study found that Tm with diameters <3 cm were significantly affected by PVE, and the impact of PVE diminished as tumor size increased.

In recent years, ^{99}Y microsphere therapy has become a widely used, effective, and safe radionuclide therapy option for primary and metastatic liver Tm. The success of this therapy depends on accurate calculation, of tumor dose, which is determined by various parameters. Prior to administration of ^{99}Y microspheres to the patient, dosimetry is performed using Tc-99m-MAA with SPECT/CT imaging. When dosimetric calculations rely solely on SPECT images, the regions of interest VOIs may appear larger than their actual size due to radiotracer spill-out (17). PVE in SPECT imaging arises from the system's limited spatial resolution. It is also influenced by whether corrections such as reconstruction algorithms and collimator-detector response have been applied. PVE includes both partial volume loss and spillover from neighboring regions, and particularly for structures smaller than 2-3 times of the system's FWHM (18).

Recently, 3D-printed phantoms made of PLA material have been used. It has been reported that PLA phantoms can be filled with Tc-99m and lutetium-177 radionuclides, which are mixed with water, allowing the acquisition of their scintigraphic images. These images can then be analyzed for scatter and photon attenuation effects (19).

Studies on PVE correction in scintigraphic imaging have shown that restoration filters based on frequency-distance relationships or approaches using spatial resolution modeling depending on distance in iterative reconstruction can reduce PVE; however, complete recovery of activity is not always achievable (20,21).

Factors degrading IQ and reducing the absorbed dose to lesions have been analyzed by Pacilio et al. (22) using Monte Carlo simulations. PVE was identified as one of the most significant degrading effects in scintigraphic images, with activity loss exceeding 20% in 1.8 cm lesions. It was reported that lesions smaller than 2 cm should be excluded from voxel-based dosimetry because accurate corrections cannot be performed (23). Cheng et al. (24) reported that PVE can significantly impact the accuracy of voxel-based dosimetry due to high noise in the images, and recommended increasing the number of iterations and subsets in image reconstruction. Additionally, they noted that high activity concentration may partially correct PVE. It has also been reported that pre- or post-filtering reduces spatial resolution and increases PVE, therefore, image filtering is not recommended (8).

In studies related to PVE and scintigraphic IQ, it has been reported that contrast and CNR values, which are methods used to evaluate IQ, are affected by PVE (25). A more detrimental effect than bias caused by PVE is the significant variability PVE introduces in lesion uptake. This variability can lead to substantial differences in measured tumor uptake, depending on tumor characteristics (e.g., size and shape), technical specifications of the tomography (e.g., spatial resolution), processing methods (e.g., reconstruction algorithms), and measurement procedures. Moreover, this variability hinders the feasibility of meta-analyses based on published data, posing substantial challenges for future clinical studies (26).

Kerckhaert et al. (27) evaluated IQ using an NEMA IQ phantom with Tc-99m-MAA and reported CNR values of 7.26 and 10.3 for 10 mm and 37 mm diameter lesions, respectively. In our study, tumor doses showed good correlation with tumor volumes (R^2=0.7267). Similarly, strong correlations were observed between tumor dose and CNR (R^2=0.8), and tumor dose and contrast (R^2=0.94). For lesions with diameters of 2 cm and 5 cm, contrast and CNR values were found to be 2.03 and 3.89, respectively. These results indicate a 1.9-fold improvement in contrast and a 2.43-fold improvement in CNR, respectively, in the 5 cm lesion. The actual and SPECT/CT-derived absorbed doses for the 2 cm lesion were 15.3 Gy and 7.87 Gy while for the 5 cm lesion, they were 15.4 Gy and 13.38 Gy, respectively. These findings highlight that the error due to PVE in dose estimation decreases with increasing lesion size.

Roesink JM et al. (28) who studied the effect of PVE on tumor dose, reported that tumor doses decreased as PVE increased. Consistently, in this study, it was observed that the T/N ratios decreased with decreasing tumor size on SPECT/CT images, likely due to the effect of partial volume effect PVE.

Study Limitations

This study presents data for a single model device. It does not include data from other brands or models of gamma cameras

Conclusion

To significantly reduce the bias caused by the partial volume effect, simple but imperfect correction methods currently being utilized. Until a widely accepted correction technique is routinely implemented, great care should be taken to standardize the acquisition, processing, and analysis of imaging data. In this context, it was concluded that Tms smaller than 2 cm are significantly affected by PVE, and applying necessary corrections in dosimetric calculations will have a decisive impact on the accuracy of dosimetric results.

Ethics

Ethics Committee Approval: Since the study was conducted solely on a phantom model and did not involve any human subjects, ethical approval, informed consent, and volunteer consent forms were not required

Informed Consent: Since this study does not involve live subjects and was conducted solely on a phantom model, ethical approval, informed consent, and consent forms are not required.

Footnotes

Authorship Contributions

Surgical and Medical Practices: A.D.A., M.D., Concept: A.D.A., N.Y., S.A., Ö.D., M.D., Design: A.D.A., S.A., M.D., Data Collection or Processing: A.D.A., M.D., Analysis or Interpretation: A.D.A., M.D., Literature Search: A.D.A., N.Y., S.A., M.D., Writing: A.D.A., Ö.D., M.D.

Conflict of Interest: No conflict of interest was declared by the authors.

Financial Disclosure: The authors declared that this study has received no financial support.

References

1. Geschwind JF, Salem R, Carr BI, Soulen MC, Thurston KG, Goin KA, Van Buskirk M, Roberts CA, Goin JE. Yttrium-90 microspheres for the treatment of hepatocellular carcinoma. Gastroenterology. 2004;127:S194-S205.
2. Silva LP, Paiva E, Trombini H. Heterogeneity in dose distribution in Yttrium-90 and Holmium-166 microspheres radioembolization of hepatic tumors. Radiation Physics and Chemistry. 2025;230:1-7.
3. Salem R, Lewandowski RJ, Gates VL, Nutting CW, Murthy R, Rose SC, Soulen MC, Geschwind JF, Kulik L, Kim YH, Spreafico C, Maccauro M, Bester L, Brown DB, Ryu RK, Sze DY, Rilling WS, Sato KT, Sangro B, Bilbao JI, Jakobs TF, Ezziddin S, Kulkarni S, Kulkarni A, Liu DM, Valenti D, Hilgard P, Antoch G, Muller SP, Alsuhaibani H, Mulcahy MF, Burrel M, Real MI, Spies S, Esmail AA, Raoul JL, Garin E, Johnson MS, Benson AB 3rd, Sharma RA, Wasan H, Lambert B, Memon K, Kennedy AS, Riaz A; Technology assessment committee; ınterventional oncology task force of the society of ınterventional radiology. Research reporting standards for radioembolization of hepatic malignancies. J Vasc Interv Radiol. 2011;22:265-278.
4. Salem R, Thurston KG. Radioembolization with 90Yttrium microspheres: a state-of-the-art brachytherapy treatment for primary and secondary liver malignancies. Part 1: technical and methodologic considerations. J Vasc Interv Radiol. 2006;17:1251-1278.
5. Miller FH, Lopes Vendrami C, Gabr A, Horowitz JM, Kelahan LC, Riaz A, Salem R, Lewandowski RJ. Evolution of radioembolization in treatment of hepatocellular carcinoma: a pictorial review. Radiographics. 2021;41:1802-1818.
6. Lambert B, Mertens J, Sturm EJ, Stienaers S, Defreyne L, D'Asseler Y. 99mTc-labelled macroaggregated albumin (MAA) scintigraphy for planning treatment with 90Y microspheres. Eur J Nucl Med Mol Imaging. 2010;37:2328-2333.
7. Jadoul A, Bernard C, Lovinfosse P, Gérard L, Lilet H, Cornet O, Hustinx R. Comparative dosimetry between ^{99m}Tc-MAA SPECT/CT and ^{90}Y PET/CT in primary and metastatic liver tumors. Eur J Nucl Med Mol Imaging. 2020;47:828-837.
8. Dawson LA, Ten Haken RK. Partial volume tolerance of the liver to radiation. Semin Radiat Oncol. 2005;15:279-283.
9. Chiesa C, Sjogreen-Gleisner K, Walrand S, Strigari L, Flux G, Gear J, Stokke C, Gabina PM, Bernhardt P, Konijnenberg M. EANM dosimetry committee series on standard operational procedures: a unified methodology for ^{99m}Tc-MAA pre- and ^{90}Y peri-therapy dosimetry in liver radioembolization with ^{90}Y microspheres. EJNMMI Phys. 2021;8:77.
10. Yeyin N, Kesmezacar FF, Tunçman D, Demir Ö, Uslu-Beşli L, Günay O, Demir M. Hepatopulmonary shunt ratio verification model for transarterial radioembolization. Curr Radiopharm. 2024;17:276-284.
11. Dieckens D, Lavalaye J, Romijn L, Habraken J. Contrast-noise-ratio (CNR) analysis and optimisation of breast-specific gamma imaging (BSGI) acquisition protocols. EJNMMI Res. 2013;3:21.
12. Dezarn WA, Cessna JT, DeWerd LA, Feng W, Gates VL, Halama J, Kennedy AS, Nag S, Sarfaraz M, Sehgal V, Selwyn R, Stabin MG, Thomadsen BR, Williams LE, Salem R; American Association of Physicists in Medicine. Recommendations of the American Association of Physicists in Medicine on dosimetry, imaging, and quality assurance procedures for 90Y microsphere brachytherapy in the treatment of hepatic malignancies. Med Phys. 2011;38:4824-4845.
13. Thurnheer R, Engel H, Weder W, Stammberger U, Laube I, Russi EW, Bloch KE. Role of lung perfusion scintigraphy in relation to chest computed tomography and pulmonary function in the evaluation of candidates for lung volume reduction surgery. Am J Respir Crit Care Med. 1999;159:301-310.
14. Elschot M, Nijsen JF, Lam MG, Smits ML, Prince JF, Viergever MA, van den Bosch MA, Zonnenberg BA, de Jong HW. (^{99}m)Tc-MAA overestimates the absorbed dose to the lungs in radioembolization: a quantitative evaluation in patients treated with ^{166}Ho-microspheres. Eur J Nucl Med Mol Imaging. 2014;41:1965-1975.
15. Tafti BA, Padia SA. Dosimetry of Y-90 microspheres utilizing Tc-99m SPECT and Y-90 PET. Semin Nucl Med. 2019;49:211-217.
16. Kafrouni M, Allimant C, Fourcade M, Vauclin S, Guiu B, Mariano-Goulart D, Ben Bouallègue F. Analysis of differences between 99m Tc-MAA SPECT-and 90 Y- microsphere PET-based dosimetry for hepatocellular carcinoma selective internal radiation therapy. EJNMMI Research. 2019;9:1-9.
17. Du Y, Tsui BM, Frey EC. Partial volume effect compensation for quantitative brain SPECT imaging. IEEE Trans Med Imaging. 2005;24:969-976.
18. Grings A, Jobic C, Kuwert T, Ritt P. The magnitude of the partial volume effect in SPECT imaging of the kidneys: a phantom study. EJNMMI Phys. 2022;9:18.
19. Pretorius PH, King MA, Pan TS, de Vries DJ, Glick SJ, Byrne CL. Reducing the influence of the partial volume effect on SPECT activity quantitation

with 3D modelling of spatial resolution in iterative reconstruction. Phys Med Biol. 1998;43:407-420.

20. Yokoi T, Shinohara H, Onishi H. Performance evaluation of OSEM reconstruction algorithm incorporating three-dimensional distance-dependent resolution compensation for brain SPECT: a simulation study. Ann Nucl Med. 2002;16:11-18.
21. Pacilio M, Ferrari M, Chiesa C, Lorenzon L, Mira M, Botta F, Becci D, Torres LA, Perez MC, Gil AV, Basile C, Ljungberg M, Pani R, Cremonesi M. 3D dosimetry treatment planning with 99mTc macroaggregated albumin SPECT in radioembolization with 90Y microspheres: a Monte Carlo study of the impact on absorbed dose distributions of attenuation and scatter corrections using the patient relative calibration methodology. Med Phys. 2016;43:4053-4064.
22. Chiesa C, Mira M, Maccauro M, Spreafico C, Romito R, Morosi C, Camerini T, Carrara M, Pellizzari S, Negri A, Aliberti G, Sposito C, Bhoori S, Facciorusso A, Civelli E, Lanocita R, Padovano B, Migliorisi M, De Nile MC, Seregni E, Marchianò A, Crippa F, Mazzaferro V. Radioembolization of hepatocarcinoma with (90)Y glass microspheres: development of an individualized treatment planning strategy based on dosimetry and radiobiology. Eur J Nucl Med Mol Imaging. 2015;42:1718-1738.
23. Cheng L, Hobbs RF, Segars PW, Sgouros G, Frey EC. Improved dose-volume histogram estimates for radiopharmaceutical therapy by optimizing quantitative SPECT reconstruction parameters. Phys Med Biol. 2013;58:3631-3647.
24. Kästner D, Braune A, Brogsitter C, Freudenberg R, Kotzerke J, Michler E. Gamma camera imaging characteristics of ^{166}Ho and ^{99m}Tc used in selective ınternal radiation therapy. EJNMMI Phys. 2024;11:35.
25. Soret M, Bacharach SL, Buvat I. Partial-volume effect in PET tumor imaging. J Nucl Med. 2007;48:932-945.
26. Kerckhaert CEM, de Jong HWAM, Meddens MBM, van Rooij R, Smits MLJ, Rakvongthai Y, Dietze MMA. Subtraction of single-photon emission computed tomography (SPECT) in radioembolization: a comparison of four methods. EJNMMI Phys. 2024;11:72.
27. Roesink JM, Moerland MA, Hoekstra A, Van Rijk PP, Terhaard CH. Scintigraphic assessment of early and late parotid gland function after radiotherapy for head-and-neck cancer: a prospective study of dose-volume response relationships. Int J Radiat Oncol Biol Phys. 2004;58:1451-1460.